Chapter 1

A Guided Tour

1.1. Introduction

In this first chapter[1], we propose an overview with a short introduction to wavelets. We will focus on several applications with priority given to aspects related to statistics or signal and image processing. Wavelets are thus observed in action without preliminary knowledge. The chapter is organized as follows: apart from the introduction to wavelets, each section centers on a figure around which a comment is articulated.

First of all, the concept of wavelets and their capacity to describe the local behavior of signals at various time scales is presented. Discretizing time and scales, we then focus on orthonormal wavelet bases making it possible at the same time:

– to supplement the analysis of irregularities with those of local approximations;

– to organize wavelets by scale, from the finest to the coarsest;

– to define fast algorithms of linear complexity.

Next we treat concrete examples of real one-dimensional signals and then two-dimensional (images) to illustrate the three following topics:

– *analysis* or how to use the wavelet transform to scan the data and determine the pathways for a later stage of processing. Indeed, wavelets provide a framework for signal decomposition in the form of a sequence of signals known as approximation

1 This chapter is a translated, slightly modified version of the [MIS 98] article published in the French scientific journal, *Journal de la Société Française de Statistique*, which the authors thank for their kind authorization.

signals with decreasing resolution supplemented by a sequence of additional touches called details. A study of an electrical signal illustrates this point;

– *denoising* or estimation of functions. This involves reconstituting the signal as well as possible on the basis of the observations of a useful signal corrupted by noise. The methods based on wavelet representations yield very simple algorithms that are often more powerful and easy to work with than traditional methods of function estimation. They consist of decomposing the observed signal into wavelets and using thresholds to select the coefficients, from which a signal is synthesized. The ideas are introduced through a synthetic Doppler signal and are then applied to the electrical signal;

– *compression* and, in particular, image compressions where wavelets constitute a very competitive method. The major reason for this effectiveness stems from the ability of wavelets to generally concentrate signal energy in few significantly non-zero coefficients. Decomposition structure is then sparse and can be coded with very little information. These methods prove useful for signals (an example thereof is examined), as well as for images. The use of wavelets for images is introduced through a real image, which is then compressed. Lastly, a fingerprint is compressed using wavelet packets which generalize wavelets.

The rapid flow of these topics focuses on main ideas and merely outlines the many theoretical and practical aspects tackled. These are detailed in other chapters of this book: Chapter 2 for the mathematical framework, Chapters 5, 6 and 8 for the analysis, and Chapters 7 and 8 for denoising and compression.

1.2. Wavelets

1.2.1. *General aspects*

Let ψ be a sufficiently regular and well localized function. This function $\psi \in L^1 \cap L^2$ will be called a wavelet if it verifies the following admissibility condition in the frequency domain:

$$\int_{\mathbb{R}^+} \frac{\left|\hat{\psi}(\omega)\right|^2}{|\omega|} d\omega = \int_{\mathbb{R}^-} \frac{\left|\hat{\psi}(\omega)\right|^2}{|\omega|} d\omega < +\infty$$

where $\hat{\psi}$ indicates the Fourier transform of ψ. This condition involves, in particular, that the wavelet integrates to zero. This basic requirement is often

reinforced by requiring that the wavelet has m vanishing moments, i.e. verify $\int_{\mathbb{R}} t^k \psi(t)\,dt = 0$ for $k = 0,\ldots,m$.

A sufficient admissibility condition that is much simpler to verify is, for a real wavelet ψ, provided by:

$$\psi\ ,\ \psi \in L^1 \cap L^2\ ,\ t\,\psi \in L^1 \text{ and } \int_{\mathbb{R}} \psi(t)\,dt = 0$$

To consolidate the ideas let us say that during a certain time a wavelet oscillates like a wave and is then localized due to a damping. The oscillation of a wavelet is measured by the number of vanishing moments and its localization is evaluated by the interval where it takes values significantly different from zero.

From this single function ψ using translation and dilation we build a family of functions that form the basic atoms:

$$\psi_{a,b}(t) = \frac{1}{\sqrt{a}}\psi\left(\frac{t-b}{a}\right) \qquad a \in \mathbb{R}^+, b \in \mathbb{R}$$

For a function f of finite energy we define its continuous wavelet transform by the function C_f:

$$C_f(a,b) = \int_{\mathbb{R}} f(t)\,\overline{\psi_{a,b}(t)}\,dt$$

Calculating this function C_f amounts to analyzing f with the wavelet ψ. The function f is then described by its wavelet coefficients $C_f(a,b)$, where $a \in \mathbb{R}^+$ and $b \in \mathbb{R}$. They measure the fluctuations of function f at scale a. The trend at scale a containing slower evolutions is essentially eliminated in $C_f(a,b)$. The analysis in wavelets makes a local analysis of f possible, as well as the description of scale effects comparing the $C_f(a,b)$ for various values of a. Indeed, let us suppose that ψ is zero outside of $[-M,+M]$, so $\psi_{a,b}$ is zero outside the interval $[-Ma+b, Ma+b]$. Consequently, the value of $C_f(a,b)$ depends on the values of f in a neighborhood of b with a length proportional to a.

In this respect let us note that the situation with wavelets differs from the Fourier analysis, since the value of the Fourier transform $\hat{f}(\omega)$ of f in a point ω depends on the values of f on the entire $\mathbb{R}$. Qualitatively, large values of $C_f(a,b)$ provide information on the local irregularity of f around position b and at scale a. In this

sense, wavelet analysis is an analysis of the fluctuations of f at all scales. Additional information on quantifying the concept of localization and the comparison between the Fourier and wavelet analyses may be found in [MAL 98] or in [ABR 97].

The continuous transform (see, for example, [TOR 95] or [TEO 98]) defined above makes it possible to characterize the Holderian regularity of functions and its statistical use for the detection of transient phenomena or change-points fruitful (see Chapter 6).

In many situations (and throughout this chapter) we limit ourselves to the following values of a and b:

$$a = 2^j,\ b = k2^j = ka \text{ for } (j,k) \in \mathbb{Z}^2$$

In this case and for wavelets verifying stronger properties than merely the admissibility condition – in particular, in the orthogonal case (specified below), which we shall consider from now on – a function called a scaling function and denoted φ is associated with ψ. We dilate and translate it as ψ. On the whole, the φ function is for local approximations what the ψ function is for fluctuations around the local approximation, also called the local trend.

We then define the basic atoms of wavelets which are also sometimes called wavelets:

$$\begin{cases} \psi_{j,k}(x) = 2^{-j/2}\psi(2^{-j}x - k), & \text{for} \quad (j,k) \in \mathbb{Z}^2 \\ \varphi_{j,k}(x) = 2^{-j/2}\varphi(2^{-j}x - k), & \text{for} \quad (j,k) \in \mathbb{Z}^2 \end{cases}$$

In this context, the wavelet coefficients of a signal s are provided by

$$\alpha_{j,k} = \int_{\mathbb{R}} s(t)\psi_{j,k}(t)\,dt$$

and, under certain conditions (verified for orthogonal wavelets), these coefficients are enough to reconstruct the signal by:

$$s(t) = \sum_{j\in\mathbb{Z}} \sum_{k\in\mathbb{Z}} \alpha_{j,k}\, \psi_{j,k}(t)$$

The existence of a function ψ such that the family $\left\{\psi_{j,k}\right\}_{(j,k)\in\mathbb{Z}^2}$ is an orthonormal basis of $L^2(\mathbb{R})$ is closely related to the concept of multi-resolution analysis (MRA) (see [MEY 90], [MAL 89] and [MAL 98], and also Chapter 2). An MRA of the space $L^2(\mathbb{R})$ of finite energy signals is a sequence $\left\{V_j\right\}_{j\in\mathbb{Z}}$ of nested closed subspaces:

$$\cdots \subset V_2 \subset V_1 \subset V_0 \subset V_{-1} \subset V_{-2} \subset \cdots$$

of $L^2(\mathbb{R})$ whose intersection is reduced to $\{0\}$ and the union is dense in $L^2(\mathbb{R})$. These spaces are all deduced from the "central" space V_0 by contraction (for $j < 0$) or dilation (for $j > 0$), i.e.:

$$f(t) \in V_j \Leftrightarrow f(2t) \in V_{j-1} \quad \text{for} \quad j \in \mathbb{Z}$$

Lastly, there is a function φ of V_0, which generates V_0 by integer translations, that is so that:

$$V_0 = \left\{ f \in L^2(\mathbb{R}) \mid f(t) = \sum_{k\in\mathbb{Z}} e_k \varphi(t-k), \left(e_k\right) \in l^2(\mathbb{Z}) \right\}$$

where the φ function is the scaling function introduced above.

Subspaces $\{V_j\}_{j\in\mathbb{Z}}$ of MRA are used as approximation (or trend) spaces. In addition, we also define detail spaces noted as $\{W_j\}_{j\in\mathbb{Z}}$. For fixed $j \in \mathbb{Z}$, the W_j space is the orthogonal complement of V_j in V_{j-1}:

$$V_{j-1} = V_j \oplus W_j \quad \text{for} \quad j \in \mathbb{Z}$$

An element of the approximation space of level $j-1$ is decomposed into an approximation at level j, which is less accurate, and a detail at level j.

The integer translates of φ $\{\varphi_{j,k}\}_{k\in\mathbb{Z}}$ generate V_j while those of ψ $\{\psi_{j,k}\}_{k\in\mathbb{Z}}$ generate W_j. Since $L^2(\mathbb{R}) = \bigoplus_{j\in\mathbb{Z}} W_j$, any signal is the sum of all its details and $\{\psi_{j,k}\}_{(j,k)\in\mathbb{Z}^2}$ form an orthonormal wavelet basis of $L^2(\mathbb{R})$. Thus, $\alpha_{j,k}$ is the coefficient associated with $\psi_{j,k}$ in the orthogonal projection of s onto W_j.

The respective roles of the φ and ψ functions, as well as the concepts of detail and approximation, will be illustrated below using examples. Let us now examine an "orthogonal" wavelet.

1.2.2. *A wavelet*

Figure 1.1 relates to the wavelet noted *db4* after I. Daubechies.

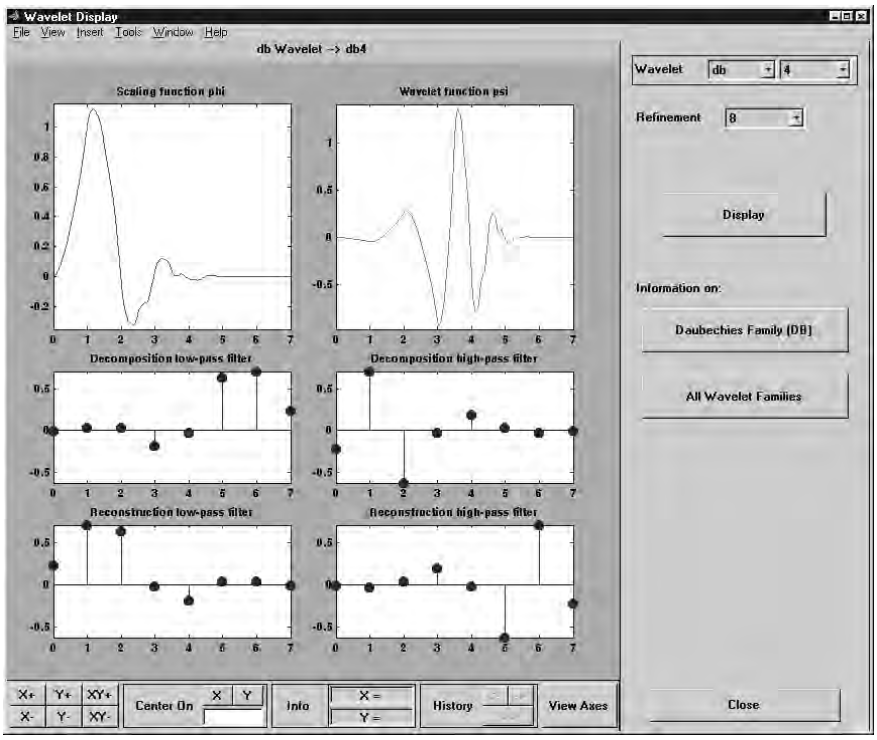

Figure 1.1. *The wavelet noted db4 after I. Daubechies*

At the top, from left to right, we find the scaling function and then the wavelet. As can be seen, the wavelet ψ oscillates and integrates to zero, while the scaling function φ oscillates less and has a positive integral (in fact, equal to 1). Consequently, calculating the scalar product of a function or a signal with a wavelet makes it possible to analyze the fluctuations of the signal around a local average provided by the calculation of the scalar product of the signal and the scaling function.

Below we provide the four filters used to carry out the calculation of coefficients by a fast algorithm due to S. Mallat (see Chapter 3). These filters go by pairs. Two are associated with the scaling function φ and they appear in the first column, while the two other filters, in the second column, are associated with the wavelet ψ .

In a column we pass from one filter to another taking the mirror filter, and in a row we pass from one filter to another taking the mirror filter and multiplying the even-indexed terms by –1. Thus, just one of these four filters is enough to produce all the others. Similarly, we can show that on the basis of a given MRA and, thus, of the scaling function, we can construct the wavelet.

The filters appear in the relations concerning the basic functions associated with successive levels. These are the equations on two following scales:

$$\varphi_{j+1,0} = \sum_{k\in\mathbb{Z}} h_k \varphi_{j,k} \quad \text{and} \quad \psi_{j+1,0} = \sum_{k\in\mathbb{Z}} g_k \varphi_{j,k}$$

The sequence *h* determines the filters of the first column and the sequence *g* determines those of the second column.

The wavelet presented in Figure 1.1 forms part of a family of *dbn* wavelets indexed by $n \in \mathbb{N}^*$ introduced by I. Daubechies in 1990 (see Chapter 4 for the construction). The wavelet *db1* is simply the Haar wavelet.

The main properties of the *dbn* wavelet are as follows:

– it is an orthogonal wavelet, associated with an MRA;

– it has compact support [0, $2n - 1$] and the associated filters are of length $2n$;

– the number of vanishing moments is n and, in general, it is far from symmetric;

– the regularity is 0, 2*n* when n is sufficiently large.

1.2.3. *Organization of wavelets*

Wavelets are thus organized using two parameters:

– time k making it possible to translate the forms for a given level;

– scale 2^j making it possible to pass from a level j to the immediately lower level in the underlying tree represented in Figure 1.2.

In the first column of the figure we find the dyadic dilates (2 times, 4 times, 8 times, etc.) of the scaling function φ and in the second column, those of the wavelet ψ.

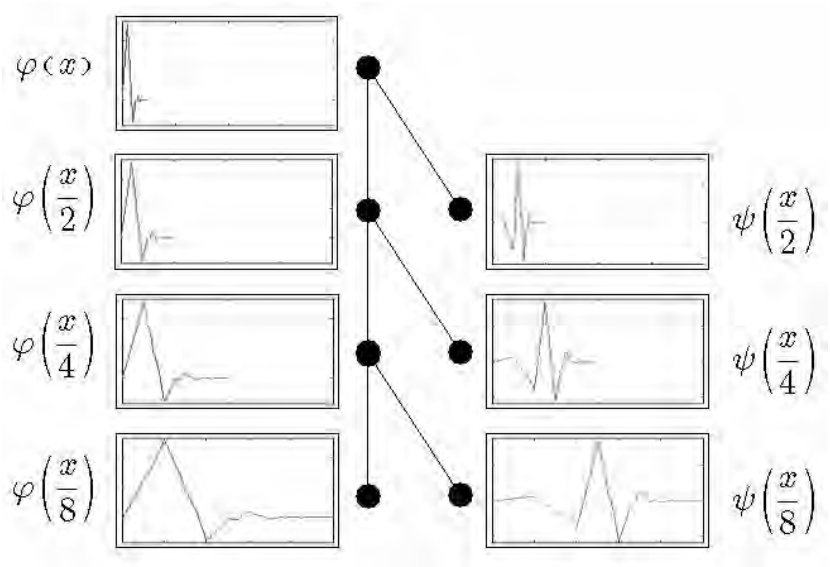

Figure 1.2. *Organization of wavelets*

The functions in the first column are used for calculating the coefficients of approximation $\beta_{j,k} = \int_{\mathbb{R}} s(t)\varphi_{j,k}(t)dt$, which define local averages of the signal $s(t)$. The signal $A_j(t) = \sum_{k\in\mathbb{Z}} \beta_{j,k}\varphi_{j,k}(t)$ is an approximation.

The functions in the second column are associated with the calculation of wavelet coefficients $\alpha_{j,k} = \int_{\mathbb{R}} s(t)\psi_{j,k}(t)dt$, which relate to the differences between two successive local averages. These are the final touches (we shall call them details) of the form:

$$D_j(t) = \sum_{k\in\mathbb{Z}} \alpha_{j,k}\psi_{j,k}(t)$$

We therefore have four kinds of objects:

– detail coefficients $\alpha_{j,k} = \int_{\mathbb{R}} s(t)\psi_{j,k}(t)dt$, which are also wavelet coefficients enabling us to define the details;

– detail signals themselves: $D_j(t) = \sum_{k\in\mathbb{Z}} \alpha_{j,k}\psi_{j,k}(t)$;

– approximation coefficients: $\beta_{j,k} = \int_{\mathbb{R}} s(t)\varphi_{j,k}(t)\,dt$ making it possible to calculate the approximations;

– approximation signals themselves: $A_j(t) = \sum_{k\in\mathbb{Z}} \beta_{j,k}\,\varphi_{j,k}(t)$.

Detail and approximation signals are related to t, the time of the original signal, whereas the coefficients (the $\alpha_{j,k}$ and the $\beta_{j,k}$) of the level j are in dyadic time $2^j\mathbb{Z}$. The details and approximations are interpreted in terms of the orthogonal projection onto spaces W_j and V_j, respectively. For a signal s, if we compare the values of the signal to the coefficients $\left\{\beta_{0,k}\right\}_{k\in\mathbb{Z}}$ in V_0, the $\left\{\alpha_{j,k}\right\}_{k\in\mathbb{Z}}$ and $\left\{\beta_{j,k}\right\}_{k\in\mathbb{Z}}$ are the coefficients of s with respect to the bases of W_j and V_j respectively; while D_j and A_j are elements of spaces W_j and V_j, considered as functions of V_0.

1.2.4. *The wavelet tree for a signal*

Such a tree is presented in Figure 1.3. At its root we find a signal s (we may also say a time series). The tree can be read in various ways. The first column yields three approximations, from the finest A_1 to the coarsest A_3, as may be realized focusing on the end of the signal. The differences between two successive approximations are captured in the details denoted D_1 to D_3. More precisely, we have $D_1 = s - A_1$, $D_2 = A_1 - A_2$ and, thus, $s = A_2 + D_2 + D_1$.

Let us return to the case of a signal s, which is in continuous time. Starting from the equality $s = \sum_{j\in\mathbb{Z}}\sum_{k\in\mathbb{Z}} \alpha_{j,k}\,\psi_{j,k}$, meaning that we can reconstruct the signal on from its coefficients $\alpha_{j,k}$, we may use it to define the detail at level j differently. Let us fix j and sum up using k. Again we find the detail D_j:

$$D_j = \sum_{k\in\mathbb{Z}} \alpha_{j,k}\,\psi_{j,k}$$

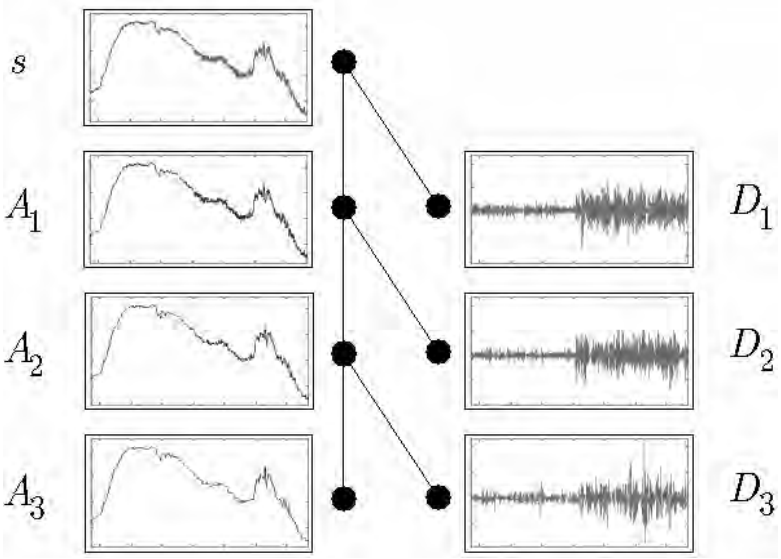

Figure 1.3. *The wavelet tree for a signal*

Let us then sum up using j. We rediscover that the signal is the sum of its details:

$$s = \sum_{j \in \mathbb{Z}} D_j$$

The details are defined. Let us now take a reference level marked J ($J = 3$ in this example). There are two kinds of details: those associated with the indices $j \leq J$ corresponding to the scales $a = 2^j \leq 2^J$, which are finer details than the resolution corresponding to J; and those for which $j > J$, are coarser. Let us aggregate the latter:

$$A_J = \sum_{j > J} D_j$$

This sum defines what will be referred to as the approximation at level J of the signal s. Moreover:

$$s = A_J + \sum_{j \leq J} D_j$$

This relation means that s is the sum of its approximation A_J and of the finer details. It can be deduced from it that the approximations are linked by:

$$A_{J-1} = A_J + D_J$$

In the orthogonal case, the family $\left\{\psi_{j,k}\right\}_{j,k \in \mathbb{Z}}$ is orthogonal and we have:

- A_J is orthogonal to $D_J, D_{J-1}, D_{J-2}, \cdots$;
- s is the sum of two orthogonal signals: A_J and $\sum_{j \leq J} D_j$;
- the quality Q_J of the approximation of s by A_J is equal to $Q_J = \frac{\|A_J\|^2}{\|s\|^2}$ and we have $Q_{J-1} = Q_J + \frac{\|D_J\|^2}{\|s\|^2}$.

1.3. An electrical consumption signal analyzed by wavelets

As a first example we consider a minute per minute record of the electrical consumption of France; the problem is presented in detail in [MIS 94].

In Figure 1.4 we find, from top to bottom, the original signal (**s**), the approximation at level 5 ($\mathbf{a_5}$) and the details from the coarsest level ($\mathbf{d_5}$) to the finest level ($\mathbf{d_1}$). All the signals are expressed in the same of time unit, which allows a synchronous reading of all the graphs. The wavelet used is *db3*.

The analyzed signal represents to the nearest transformation three days of electrical consumption during summer in France. The three days are Thursday followed by Friday, having very similar shape and amplitude, then Saturday, which

has a much lower average level due to the start of the weekend and ebbing economic activity. We may thus reinterpret the time scales corresponding to each level.

Ignoring the effects of wavelet choice, we can roughly state that $\mathbf{d_1}$ contains the components of the signal of period between 1 and 2 minutes, $\mathbf{d_2}$ those of period between 2 and 4 minutes and so on until $\mathbf{d_5}$ which contains the components of the signal of period between 16 and 32 minutes. The $\mathbf{a_5}$ approximation contains signal components of period greater than 32 minutes.

A quick examination shows that:

– the analysis makes it possible to track possible outliers, which are detected thanks to the very large values of $\mathbf{d_1}$ around the position 1,200;

– in the graphs we can distinguish the details $\mathbf{d_1}$ and $\mathbf{d_2}$ (measurement and state noises whose amplitude is low in normal circumstances) which yield details oscillating quickly around 0;

– on the contrary we isolate the period of sensor failure corresponding to the long sequence of abnormally large values of $\mathbf{d_1}$, $\mathbf{d_2}$ and, more slightly, $\mathbf{d_3}$, between the position 2,500 and the position 3,500. We have here an additional noise;

– moreover, we notice that in the details $\mathbf{d_4}$ and $\mathbf{d_5}$ we no longer distinguish this period, and the difference due to an exceptional sensors noise disappears giving an indication of the frequency contents of the additional noise;

– the daily pseudo-periodicity evident in the analyzed trajectory ($\mathbf{s}$) can be read, for the scales examined, from levels 4 and 5 through the appearance of periodic patterns in the details at equally spaced positions. From that we deduce that the details $\mathbf{d_4}$ and $\mathbf{d_5}$ contain components of the useful signal as opposed to the non-informative noise. This phenomenon does not occur for the finer levels and we could believe that the details consist almost entirely of noise.

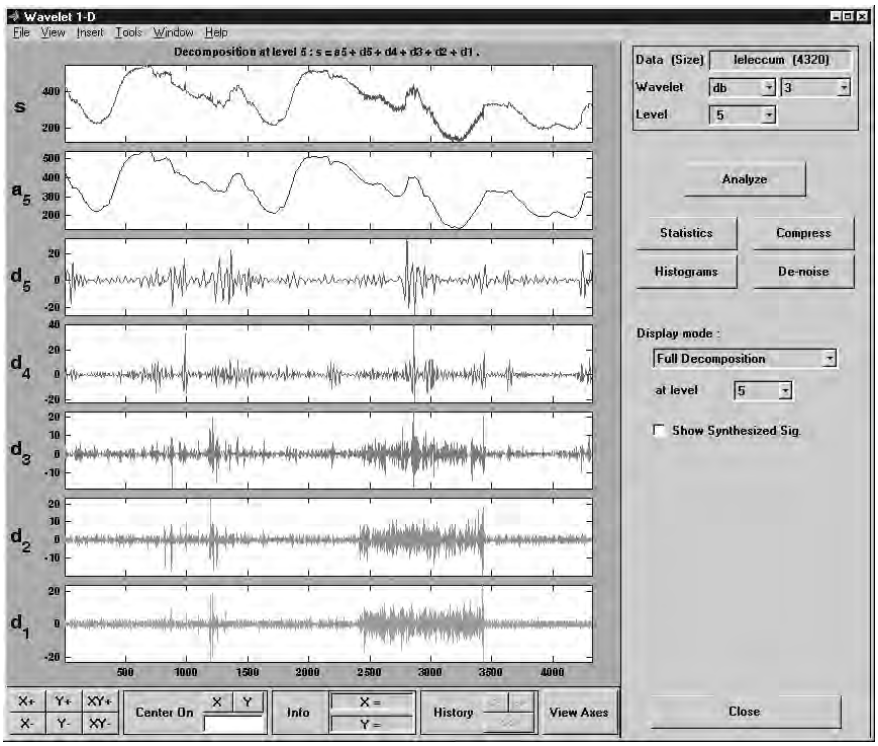

Figure 1.4. *An electrical consumption signal analyzed by wavelets*

This quick example illustrates that a simple analysis by wavelets can yield many pathways for finer processing and direct the strategy of solving classical problems, such as outlier detection, denoising reduction or signal extraction.

1.4. Denoising by wavelets: before and afterwards

Denoising is the major application of wavelets in statistics. This problem admits a very elegant solution.

In Figure 1.5 (top) we see a portion of the real noisy signal analyzed in Figure 1.4.

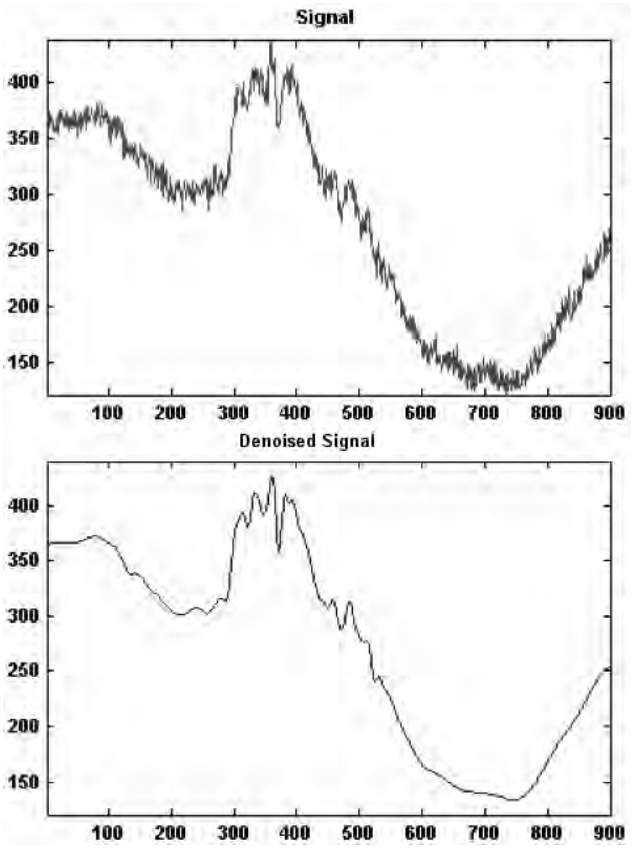

Figure 1.5. *Denoising by wavelets: before and after*

The denoised signal using wavelets is located in the lower part. It is obviously well denoised, in the zones where the signal is smooth (around positions 200 or 800, for example), as well as in the zone around instant 400 where the signal is irregular. The traditional methods of denoising are not capable of such an adaptation in time. These methods estimate the function f using the model:

$$Y_i = f(t_i) + \varepsilon_i\,, \quad t_i = \frac{i}{n}\,, \quad i = 1,\cdots,n$$

where f is unknown, $(Y_i)_i$ are observed and ε is an unobservable white noise.

1.5. A Doppler signal analyzed by wavelets

Let us first consider a simulated signal enabling us to clearly understand the spirit of the technique of denoising by wavelets (see Figure 1.6).

The screen is organized in two columns: in the first one we see the noisy signal **s**, then, in the lower part, we see the approximations from level 5 (the coarsest, $\mathbf{a_5}$) to level 1 (the finest, $\mathbf{a_1}$); in the second column at the top we see a colored version of the wavelet coefficients of levels 5 to 1 (**cfs**), followed by the noisy signal **s** and then, in the lower part, the details from level 5 (the coarsest, $\mathbf{d_5}$) to level 1 (the finest, $\mathbf{d_1}$).

The wavelet used, *sym4*, is a compactly supported almost symmetric wavelet of order 4 (see Chapter 4).

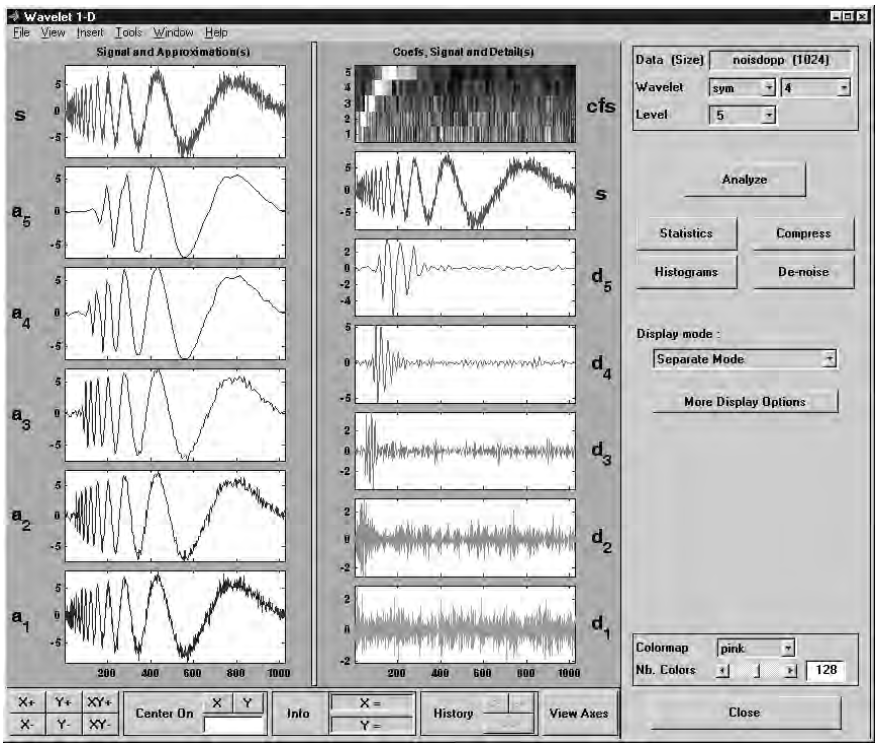

Figure 1.6. *Doppler signal analysis by wavelets*

Let us start by examining the first column and concentrate on the portion of the signal corresponding to the x-coordinates from 200 to 1,000. Starting from $\mathbf{a_1}$ let us seek, ascending, a level such that the approximation constitutes a good candidate to be an estimator of the useful signal. Levels 4 and 5 are reasonable. Nevertheless, the estimator associated with $\mathbf{a_4}$ is clearly very bad for the beginning of the signal corresponding to the x-coordinates 0 to 100. Conversely, an acceptable restitution at the beginning of the signal would result in choosing $\mathbf{a_2}$, which is visibly too noisy.

Let us now look at the details. Detail $\mathbf{d_1}$ seems to consist entirely of noise while details $\mathbf{d_2}$ to $\mathbf{d_5}$ present large values concentrated at the x-coordinates from 0 to 300. This is also visible on the graph of the wavelet coefficients (**cfs**), the largest in absolute value being the clearest. This form stems from the fact that the signal is a sinusoidal function with amplitude and period growing with time. The oscillations at the smallest scales explain the displayed details; the others are in the $\mathbf{a_5}$ approximation.

Thus, a plausible denoising strategy consists of:

– keeping an approximation such that the noise is absent or at least very attenuated ($\mathbf{a_4}$ or $\mathbf{a_5}$);

– supplementing this approximation by parts of the finer details clearly ascribable to the useful signal and rejecting the parts which are regarded as stemming from the noise.

This is precisely what the denoising by wavelets methods achieve, but in an automatic fashion. The *ad hoc* choice suggested for this particular simulated signal is that carried out by one of the most widespread methods of denoising by wavelets according to Donoho and Johnstone (see [DON 94], [DON 95a], [DON 95b]).

1.6. A Doppler signal denoised by wavelets

Let us consider Figure 1.7. The screen is organized in two columns. In the first we see wavelet coefficients from level 5 to level 1. To make them more readable, they are "repeated" 2^k times at level k (which explains the sequences of a constant gray level especially visible for $k > 3$).

In each one of these graphs we note the presence of two horizontal dotted lines: the coefficients inside the tube are zeroed by the process of denoising. In the second column at the top the noisy signal s is superimposed over the denoised signal. In the middle we find a color version of the wavelet coefficients from level 1 to 5 of the original noisy signal and in the graph at the bottom the counterpart for the

thresholded wavelet coefficients, from which the denoised signal is reconstructed. The *sym4* wavelet is used as previously.

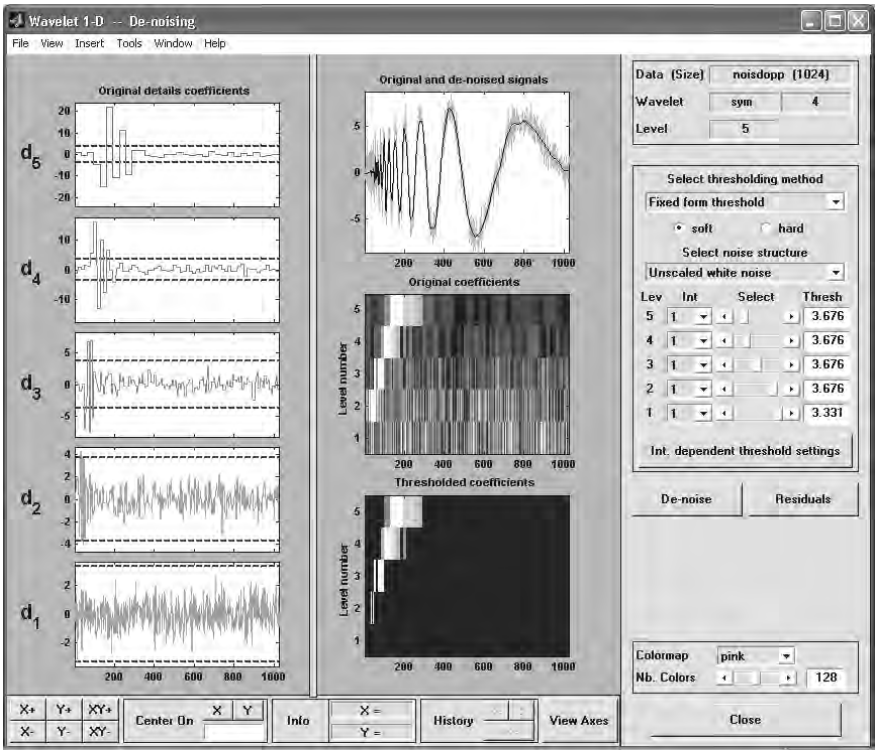

Figure 1.7. *Doppler signal denoised by wavelets*

Let us use this example to see how denoising is performed:

– all the approximation coefficients are kept, which from the onset leads to introducing the first component of the denoised signal which has the following form ($\hat{A}_d$ is not represented directly in Figure 1.7; it corresponds to the $\mathbf{a_5}$ approximation in Figure 1.6):

$$\hat{A}_d = \sum_k \hat{\beta}_{5,k} \varphi_{5,k}$$

The estimated coefficients $\hat{\beta}_{5,k}$ are simply the coefficients obtained by decomposition of the initial signal;

– only the few larger wavelet coefficients (i.e. detail coefficients) are preserved; the others are replaced by zero. In the second column we may see the coefficients before and after this thresholding operation to note the sparsity of the preserved coefficients (the black zone of the graph at the bottom corresponds to the cancelled coefficients). We thus obtain the second component of the denoised signal which has the form:

$$\hat{D}_d = \sum_{1 \leq j \leq 5} \sum_k \hat{\alpha}_{j,k} \, \psi_{j,k}$$

The estimated coefficients $\hat{\alpha}_{j,k}$ are simply the $\alpha_{j,k}$ coefficients obtained by decomposition of the initial signal and then thresholded. Many automatic methods are available for the choice of thresholds, depending on the form and the hypotheses concerning the model supposed to suitably represent the way of generating the data. We do not detail them here;

– the denoised signal is thus:

$$\hat{s}_d = \hat{A}_d + \hat{D}_d$$

It is visible that the result obtained at the top on the right has a good quality, except at the very beginning of the signal which oscillates too much on a small scale with fluctuations that are small compared to those of the noise.

1.7. An electrical signal denoised by wavelets

Let us return to the problem of denoising a real signal, which is more difficult since the nature of the noise is unknown. The method employed here takes the previous situation as a starting point by adapting the thresholding to the level.

The screen presented in Figure 1.8 is organized in two columns as in Figure 1.7. The wavelet used is *coif5*. Examining the first column we see that the coefficients of levels 1 to 3 have all been considered by this method as ascribable to the noise and that they have all been zeroed. This conforms to the conclusions of the analysis of the three day electrical load plot carried out before. On the other hand, for levels 4 and 5, the process mainly selects wavelet coefficients in the zone around the position 375, thus enabling an excellent restitution of the abrupt signal changes.

The key arguments to understand the effectiveness of these methods are as follows:

– the decomposition by wavelets is an additive analysis, consequently, the analysis of $Y_t = f(t) + \varepsilon_t$ is equal to the sum of the analyses of the signal $f(t)$ and the noise ε_t;

– if we suppose that the noise ε is white with a constant variance, the wavelet coefficients on all scales are white noise with the same variance. In addition, real signals are in many cases regular enough except in rare locations (start and end of transitory phenomena, ruptures for example), which renders the decomposition by wavelets of $f(t)$ very sparse and very well represented by the coefficients of a rather rough approximation and some large detail coefficients;

– if the irregularities generate coefficients larger than the scale of the noise, the process of thresholding only selects coefficients related to the signal provided that the scale of the noise can be suitably estimated. Lastly, the operation of thresholding always leads to regularize the signal.

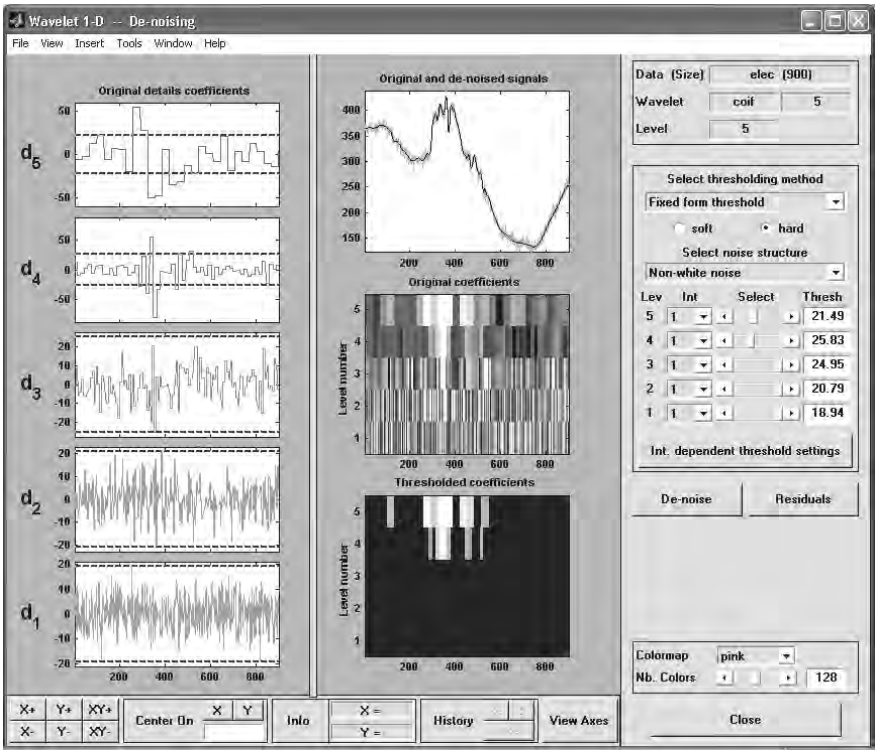

Figure 1.8. *Electrical consumption signal denoising by wavelets*

1.8. An image decomposed by wavelets

1.8.1. *Decomposition in tree form*

Let us now pass to image processing by wavelets and examine first Figure 1.9. At the top left we find the original image, in the lower part a table of images with three rows and four columns. The whole figure constitutes the tree of decomposition by wavelets; in 2D it is a quaternary tree while in 1D it is a binary tree.

In 1D the signal is decomposed into two: an approximation and a detail; in 2D the image is decomposed into four: an approximation (first column of the 3×4 table) and three details in three directions, horizontal, diagonal and vertical (three last columns of the 3×4 table). The rows of this table are indexed by levels: level 1 (the finest, noted $\mathbf{L_1}$) to level 3 (the coarsest, noted $\mathbf{L_3}$). The wavelet used here is *sym4*.

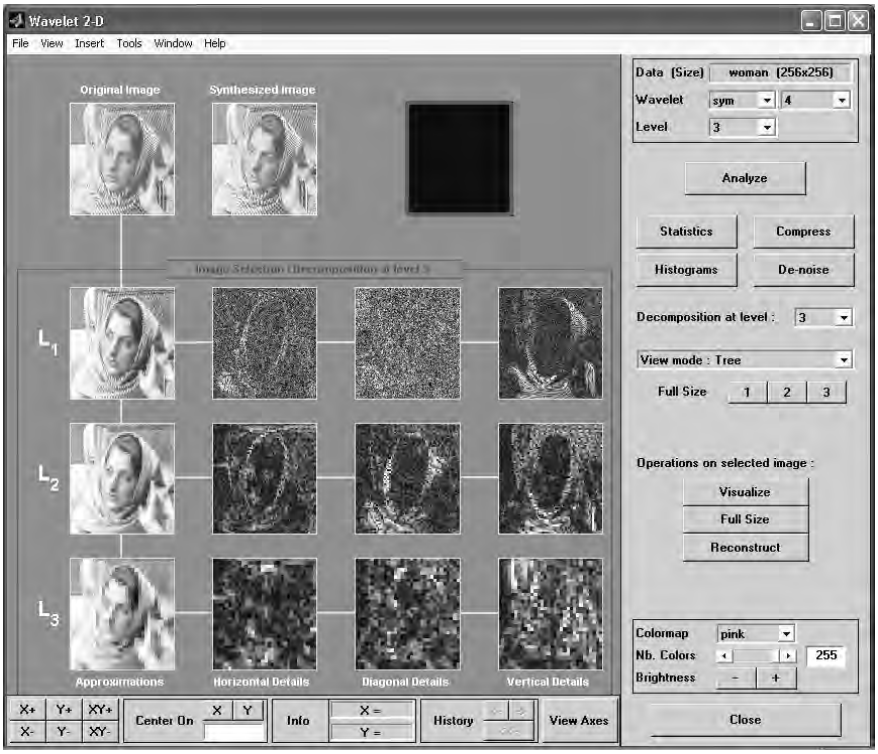

Figure 1.9. *An image ("Barbara") decomposed by wavelets. Decomposition in tree form*

Before commenting further on this screen, let us say a few words about orthogonal wavelets in 2D. These are very particular cases of wavelets, by far the most used because they lead to fast calculations, which is critical in image processing. In 1D we have two functions: φ and ψ, and the two associated filters. On this basis we produce the scaling function and the wavelets which no longer operate on the real line, but on the plane:

- $\varphi(x,y) = \varphi(x)\varphi(y)$ used to define approximations;
- $\psi_1(x,y) = \psi(x)\varphi(y)$ used to define horizontal details;
- $\psi_2(x,y) = \psi(x)\psi(y)$ used to define diagonal details;
- $\psi_3(x,y) = \varphi(x)\psi(y)$ used to define vertical details.

Algorithmic simplicity comes from the fact that it is possible to successively apply to the rows and columns of the matrix associated with the image the two filters (lowpass and highpass, respectively) useful in 1D.

Carefully examining the three approximations (in fact, their coefficients) we note that they are increasingly coarser versions of the original image.

By comparing the original image with the level 3 approximation coefficients it becomes clear that details are lost on a small scale, such as, for example, the shawl design or the weft of the cane armchair behind the face. The coefficients of detail are in general more difficult to exploit. Nevertheless, we distinguish large coefficients in the zones mentioned above, especially at level 2. We also see face features coming out in the horizontal detail of level 2.

1.8.2. *Decomposition in compact form*

The preceding representation of decomposition (see Figure 1.9) focuses on the tree structure; the one proposed in Figure 1.10 uses 2D decomposition coding.

Indeed, we find four sub-figures in this figure. The original image is top left. Let us comment on the sub-figure at the bottom right consisting of the original image decomposition coefficients.

To read this graph, we initially consider that the image is divided into quadrants. The quadrants at the bottom left, bottom right and top right are not decomposed. The three small images found represent (in the counterclockwise direction) the coefficients of vertical, diagonal and horizontal details at the finest level (level 1),

while the three following small images, located in the top left quadrant, represent the detail coefficients at level 2, and so on until we find a single small image (this is the case for the top left), which contains the approximation coefficients at the coarsest level (here 2).

The two other images, bottom left and top right, represent respectively, the image resulting from a compression process (see Figure 1.11) and the image reconstructed from only level 2 approximation coefficients. The wavelet used is still *sym4*.

The image analyzed here is a zoom of the one in Figure 1.9 and from this point of view enables finer comments. Let us concentrate on the images reproduced on the anti-diagonal of the screen. They have the same resolution as the original image and therefore can be compared directly.

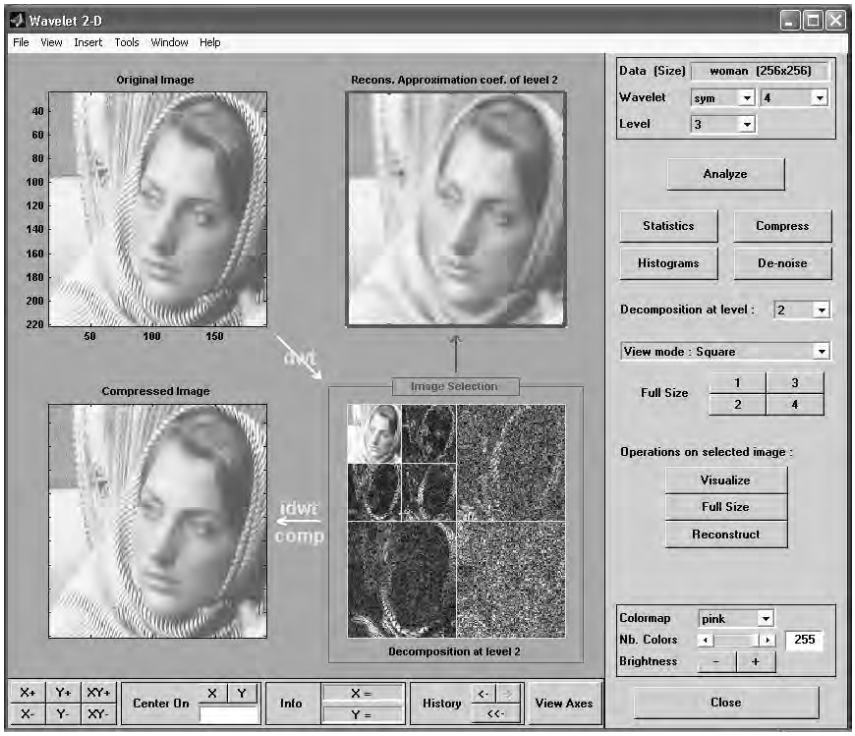

Figure 1.10. *An image ("Barbara") decomposed by wavelets. Decomposition in compact form*

Let us examine the top right image comparing it with the original image. We find the elements mentioned in the commentary on the preceding figure. The shawl design was lost in the level 2 approximation, only being discernible at scales lower

than 4 pixels. Here we recover only a rather homogenous texture with the two well restored principal folds and slightly less well-defined intermediate fold. The same holds for the armchair which is difficult to recognize. Moreover, the features of the face are fuzzier.

This general loss of contours definition can be largely improved by selectively adding coefficients of suitably selected details. After such an operation we obtain the compressed image located bottom left. It is not perfect but, nevertheless, much more accurate. Here is how it was obtained.

1.9. An image compressed by wavelets

At the top left of Figure 1.11 we find the original image, which needs to be compressed and at the top right we have the compressed image.

Below, for each level from the finest (level 1, denoted by $\mathbf{L_1}$) to the coarsest (here level 3, denoted by $\mathbf{L_3}$) we find (for each orientation: horizontal, diagonal and vertical) the grayscale histogram of the corresponding detail coefficients. In each one of these histograms we note the presence of two vertical dotted lines: the coefficients inside the vertical tube are zeroed by the process of compression.

The percentage of zeros in the representation by wavelets is more than 95%. It is an indicator of the space freed up by compression. This is a compression method with loss: approximately 98% of energy is preserved.

The criterion of energy is neither a very meaningful nor relevant indicator for the images. To evaluate the quality of restitution many numerical criteria exist but nothing is more critical than the human eye.

The method of compression is similar to that used in denoising; it is the criterion which changes. We preserve the coefficients of the roughest approximation, with which we associate the largest detail coefficients, then we reconstruct. The tuning shown in the screen presented in Figure 1.11 is manual and carried out by level and direction.

Let us examine the grayscale histograms of the detail coefficients:

– at the bottom there appear those concerning level 1. For each of the three directions all the coefficients are replaced by zero since the histogram is contained in the zone delimited by the two vertical dotted lines;

– for level 2 the strategy is a little less selective and preserves the majority of the coefficients with large absolute values;

– finally, for level 3 which is critical for image contours restitution, only the very small coefficients are eliminated, the vertical features being very close, approaching zero.

The image reconstructed by using thresholded coefficients has very good quality, despite the high percentage of coefficients replaced by zero.

These results may be improved considerably using suitably selected biorthogonal wavelets (a decomposition wavelet with a sufficient number of vanishing moments so that the representation by wavelets is the most sparse possible, associated with a dual wavelet with very regular and symmetric reconstruction in order to remove as many visual artifacts as possible). Later on we shall see an illustration thereof.

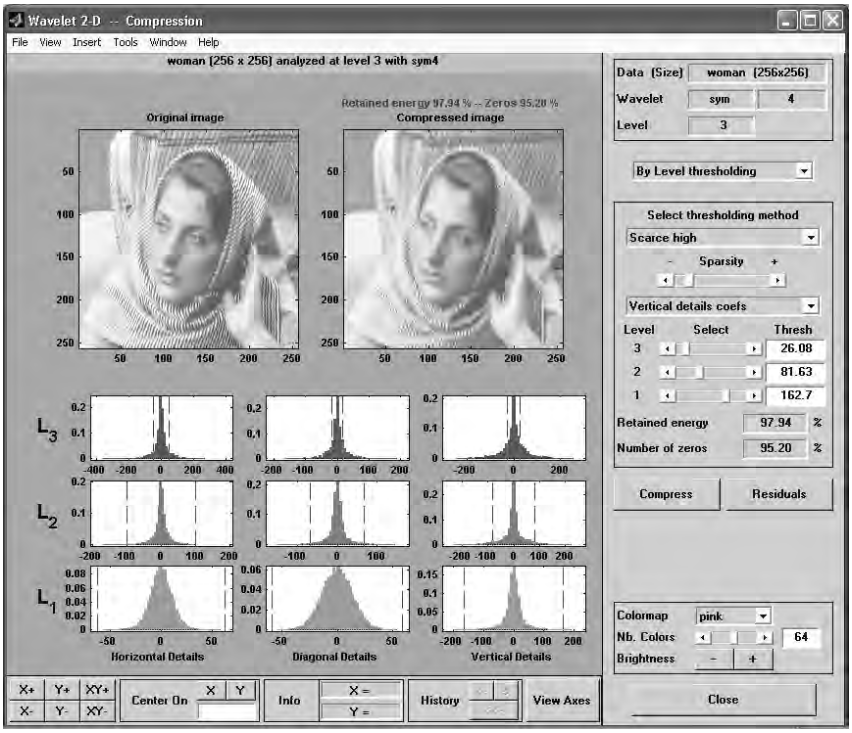

Figure 1.11. *An image ("Barbara") compressed by wavelets*

1.10. A signal compressed by wavelets

Before passing to fingerprints compression let us mention the methods of compression by wavelets of one-dimensional signals, using an artificial example.

The screen presented in Figure 1.12 is organized in two columns. In the first one we find a single graph making it possible to adjust a global threshold for the detail coefficients of the signal to be compressed (those of the approximation being preserved). All the detail coefficients whose absolute value is lower than the threshold (determined by the x-coordinate of the vertical dotted line) are zeroed by the compression. The possible values of the threshold are given by the x-axis. Two curves are drawn: one increasing which gives the percentage of zeros in the representation of the compressed signal, the other decreasing which gives the percentage of the energy preserved by the compressed signal.

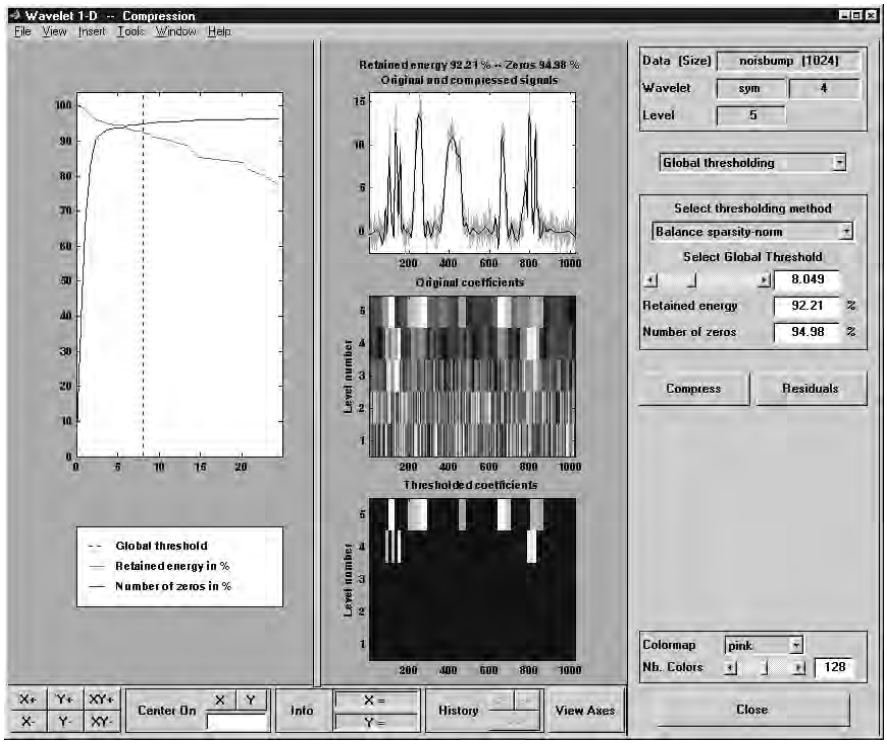

Figure 1.12. *A signal compressed by wavelets*

In the second column, the original signal is superimposed on the compressed signal. In the lower part we find a color version of the wavelet coefficients of levels 1 to 5 of the original signal and in the graph underneath is the counterpart for the thresholded wavelets coefficients, from which the compressed signal is reconstructed.

The percentage of zeros in the representation by wavelets is 95% (5% of the coefficients are preserved), for 92% of energy preserved: this stems from the fact that the signal is noisy and that therefore the very fast fluctuations are lost. The graphs (bottom right) of the coefficients before and after thresholding make it possible to notice the sparsity of the preserved coefficients. The wavelet used is *sym4*.

The compression of one-dimensional signals, although less crucial than image compression, has many applications that sometimes present a great economic interest. This is the case, for example, for companies forced to preserve the individual consumption profiles of their customers over long periods with a high degree of accuracy.

As the form of the proposed graphical interface suggests, to carry out compression by global thresholding the ideas are very close to those of denoising and the implemented algorithm is identical. It operates in three steps whose general schematic is as follows:

– decomposition by wavelets;

– we preserve the coefficients of the coarsest approximation as well as the largest wavelet coefficients in absolute value; the others are replaced by zero;

– from these modified coefficients we reconstruct the compressed signal.

1.11. A fingerprint compressed using wavelet packets

In Figure 1.13 (top right) we find the original image and (bottom left) the compressed image.

At the top left we find the wavelet packets tree and at the bottom right, the decomposition of the image to be compressed. This decomposition is obtained by decomposing into four (approximation and three details) not only the approximations but also the details. The Haar wavelet is used; the result is good but can be improved using a biorthogonal wavelet.

In Figure 1.14, at the top left we find the original image and at the top right is the compressed image. The method of compression involves a global thresholding of the wavelet packets coefficients of the image to compress. The graph underneath the original image visualizes the choice of the global threshold exactly as in 1D case. The wavelet used is a biorthogonal one.

The result is very good for a percentage of zeros of the compressed image representation equal to 95%.

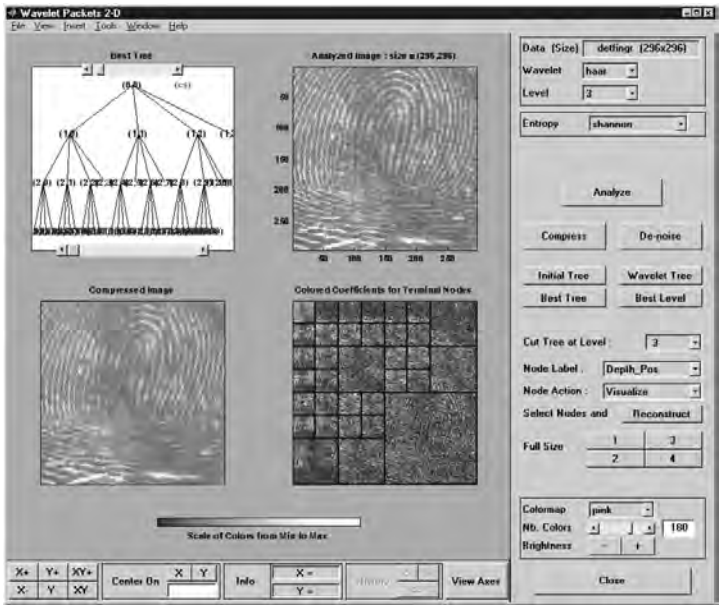

Figure 1.13. *A fingerprint analyzed and compressed by Haar wavelet packets*

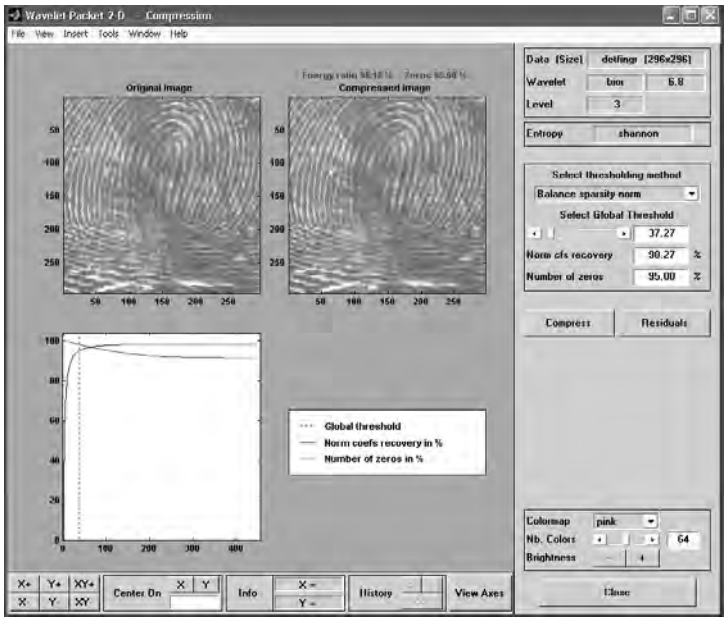

Figure 1.14. *A fingerprint compressed by biorthogonal wavelet packets*